Arch. Metall. Mater. **66** (2021), 3, 799-802

DOI: 10.24425/amm.2021.136383

HYEONHUI JO[1], YOUNG-IN LEE[1,2], MYUNG-JIN SUK[3], YOUNG-KEUN JEONG[4], SUNG-TAG OH[1,2*]

SYNTHESIS OF Y_2O_3-DISPERSED W POWDERS PREPARED BY ULTRASONIC SPRAY PYROLYSIS AND POLYMER SOLUTION ROUTE

The nano-sized Y_2O_3 dispersed W composite powder is prepared by ultrasonic spray pyrolysis of a tungsten precursor using ammonium metatungstate hydrate and a polymer addition solution method using Y-nitrate. XRD analysis for calcined powder showed the formation of WO_2 phase by partial oxidation of W powder during calcination in air. The TEM and phase analysis for further hydrogen reduction of calcined powder mixture exhibited that the W powder with a uniform distribution of Y_2O_3 nanoparticles can be successfully produced. These results indicate that the wet chemical method combined with spray pyrolysis and polymer solution is a promising way to synthesis the W-based composites with homogeneous dispersion of fine oxide particles.

Keywords: Tungsten, Y_2O_3 dispersion, Ultrasonic spray pyrolysis, Wet chemical route

1. Introduction

Due to its excellent properties such as very high melting point combined with low coefficient of thermal expansion and excellent mechanical properties at elevated temperatures, tungsten (W) is widely applied in various fields such as heating sources, light bulb filaments, aerospace materials and plasma facing wall in fusion reactors [1,2]. However, a major limitation of its use is the inherently high ductile-brittle transition temperature and serious embrittlement. In order to overcome this brittleness problem, a W-based composite material in which stable oxide fine particles are dispersed by using mechanical alloying and wet chemical processes has been developed [3-5]. However, till now the inhomogeneous distribution of oxide dispersion and the segregation of oxide particles at the grain boundaries are always great challenges for the preparation of oxide dispersion strengthened W.

Recently, the use of polymeric additives to synthesis ultrafine oxide particle with non-agglomeration characteristic has been reported [6]. This polymer solution route, which uses citric acid and polyvinyl alcohol (PVA) as chelating agents, is capable of preventing an undesirable particle growth and achieving the calcination with a lower temperature and a shorter time [7].

The aim of this work is, therefore, to investigate the synthesis of W composite powders with homogeneous dispersion of oxide nanoparticles. The fine W powders were prepared by ultrasonic spray pyrolysis of a tungsten precursor using ammonium metatungstate hydrate and hydrogen reduction. The W powders with homogeneous dispersion of Y_2O_3 on their surfaces were synthesized by a polymer addition solution method using Y-nitrate. An optimum synthesis condition is determined based on the observed microstructural characteristics of Y_2O_3-disperse W composite powders.

2. Experimental

Tungsten powder was prepared by ultrasonic spray pyrolysis using ammonium metatungstate hydrate ($(NH_4)_6H_2W_{12}O_{40}\cdot xH_2O$, >85% WO_3 basis, Sigma-Aldrich) and hydrogen reduction. At first, ammonium metatungstate hydrate with concentration of 100 mM was dissolved in distilled water of 100 mL. The precursor solution was nebulized into microdroplets by ultrasonic energy with a frequency of 1.7 MHz. Then, the aerosol droplets were sent into furnace heated to the first zone at 200°C and the second zone at 700°C using N_2 gas as carrier gas with

[1] SEOUL NATIONAL UNIVERSITY OF SCIENCE AND TECHNOLOGY,DEPARTMENT OF MATERIALS SCIENCE AND ENGINEERING, SEOUL 01811, REPUBLIC OF KOREA
[2] SEOUL NATIONAL UNIVERSITY OF SCIENCE AND TECHNOLOGY, THE INSTITUTE OF POWDER TECHNOLOGY, SEOUL 01811, REPUBLIC OF KOREA
[3] KANGWON NATIONAL UNIVERSITY, DEPARTMENT OF MATERIALS SCIENCE AND ENGINEERING, SAMCHEOK 25913, REPUBLIC OF KOREA
[4] PUSAN NATIONAL UNIVERSITY, GRADUATE SCHOOL OF CONVERGENCE SCIENCE, BUSAN 46241, REPUBLIC OF KOREA
* Corresponding author: stoh@seoultech.ac.kr

a flow rate of 2 L/min. In furnace chamber, solvent evaporation and precursor decomposition occurs, producing WO_3 powders. After then, collected powders were reduced by flowing H_2 gas at 800°C for 1 h with heating rate of 3°C/min.

To synthesis the W powder with homogeneous dispersion of Y_2O_3 nanoparticles, yttrium nitrate ($Y(NO_3)_3 \cdot 6H_2O$, Sigma-Aldrich, 237957, 99.8%) and polyvinyl alcohol (PVA, Mw 85,000-124,000) were used as the precursor and polymeric additive. A precursor solution was prepared by dissolving yttrium nitrate with the fraction of 0.5 wt% Y_2O_3 in the final composite powder in distilled water with 5 wt% PVA. As prepared W powder was then mixed with the precursor solution and stirred for 30 min. The powder mixtures were completely dried in air at 120°C for 24 h. Dried mixtures were calcined at 600°C for 5 h in air to obtain Y_2O_3 mixed powders. The powder mixtures were hydrogen-reduced at 800°C for 1 h.

Phase identification of powders was performed by X-ray Diffraction (XRD) analysis. Microstructural characteristics were examined using a field emission scanning electron microscopy (FE-SEM), a transmission electron microscopy (TEM) equipped with an energy dispersive X-ray spectroscopy (EDS) and selected area electron diffraction (SAED) patterns.

3. Results and discussion

Typical morphologies of synthesized powder by USP and hydrogen reduction are shown in Fig. 1. As clearly seen from Fig. 1(a), spherical powders less than 2 mm in size were observed in the USP powder, whereas the hydrogen reduction of powder results in the formation of a porous structure (Fig. 1(b). The XRD profiles registered for the synthesized powder are shown in Fig. 2(a). After reduction in a hydrogen atmosphere at 800°C, the powder was composed entirely of W. Neither residual W oxide nor a reaction phase were observed. Considering the reported reduction behavior [8], it is indicated that WO_3 can be completely reduced to metallic W by reduction condition used in this study.

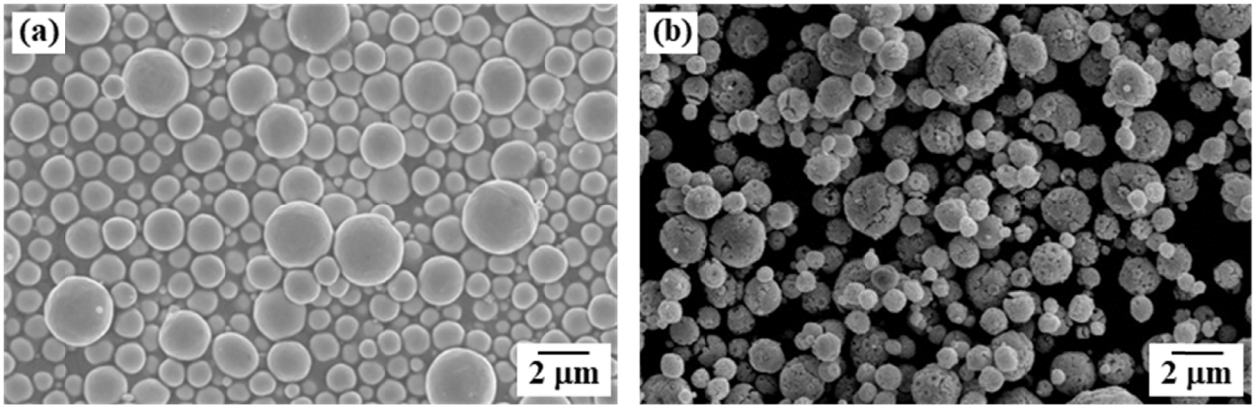

Fig. 1. SEM images of WO_3 microspheres produced from (a) USP and (b) hydrogen reduction at 800°C

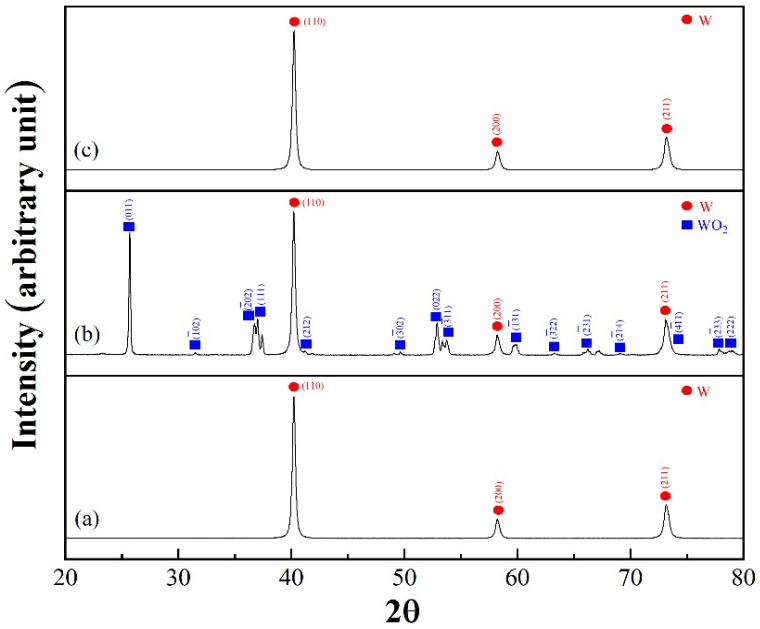

Fig. 2. XRD profiles of the powder at different stages of processing; (a) USP and hydrogen reduction at 800°C, (b) addition of Y-nitrate and calcination at 600°C and (c) W-0.5 wt% Y_2O_3 powder after hydrogen reduction at 800°C

In order to fabricate the W powders with homogenously dispersed Y_2O_3 particles, a polymer addition solution method was applied. Fig. 3 shows the SEM image for powder mixture of hydrogen-reduced W, Y-nitrate and PVA after calcination at 600°C. The synthesized powder mixture exhibited smaller powder size than that of the hydrogen-reduced W in Fig. 1. This decrease in particle size can be interpreted because the yttrium nitrate solution penetrates into the porous W powder, and the solvent is removed during drying and calcination, resulting in fracture due to crack formation.

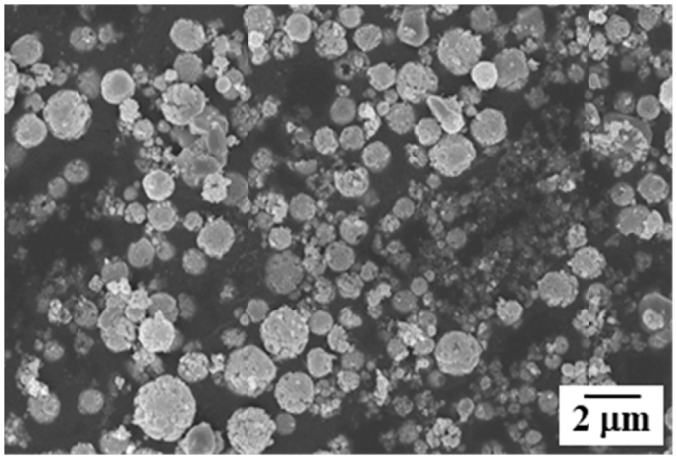

Fig. 3. SEM image for powder mixture of W and Y-nitrate after calcination at 600°C for 5 h

XRD data for the calcined powder mixture is shown in Fig. 2(b). The XRD pattern contains the characteristic peaks for the WO_2 and W. The formation of WO_2 phase is explained as being mainly due to the partial oxidation of W powder during calcination in air [9]. Meanwhile, Y_2O_3 peak was not observed in the XRD analysis, which is explained because a small volume was added below the limit of the X-ray resolution. The calcined powder mixture was further characterized by TEM accompanied by SAED. As shown in Fig. 4(a), the powder is in the form of agglomerates with nano-sized particles, and the corresponding SAED pattern could be indexed to the W, WO_2 and Y_2O_3. This result suggests that the Y_2O_3 particle was crystallized from yttrium nitrate solution during the calcination at 600°C for 5 h. However, in order to reduce the WO_2 formed during the manufacturing process to pure W, further heat treatment is required.

Fig. 2(c) and Fig. 5 show the XRD pattern and TEM-SAED results for the hydrogen-reduced powder mixture at 800°C for 1 h. As shown in Fig. 5(a), aggregates composed of fine particles of about 100 nm in size were observed. The XRD profiles registered for the pure W, whereas the SAED pattern shown in Fig. 5(b) can be indexed to the W and Y_2O_3. In order to further

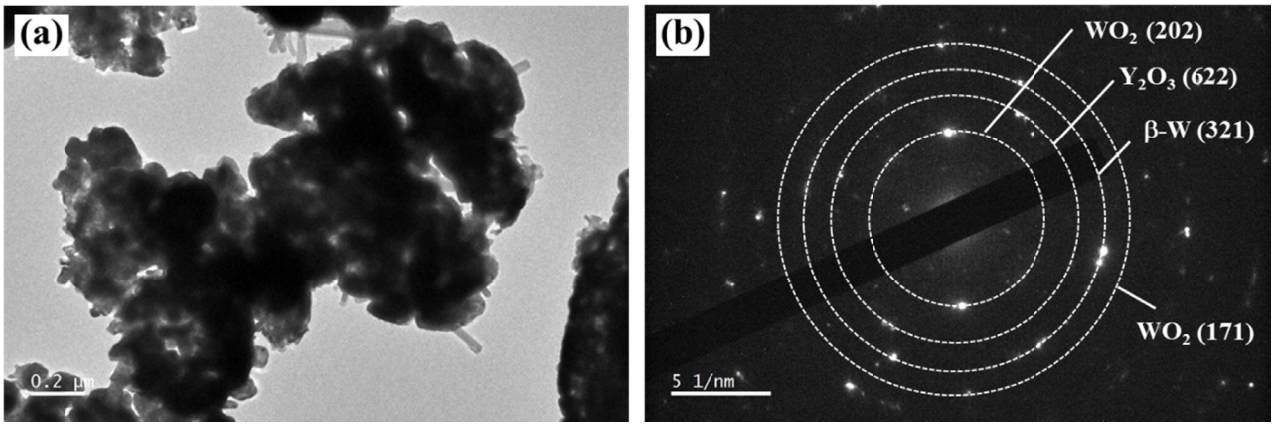

Fig. 4. TEM image and SAED pattern of calcined powder mixture

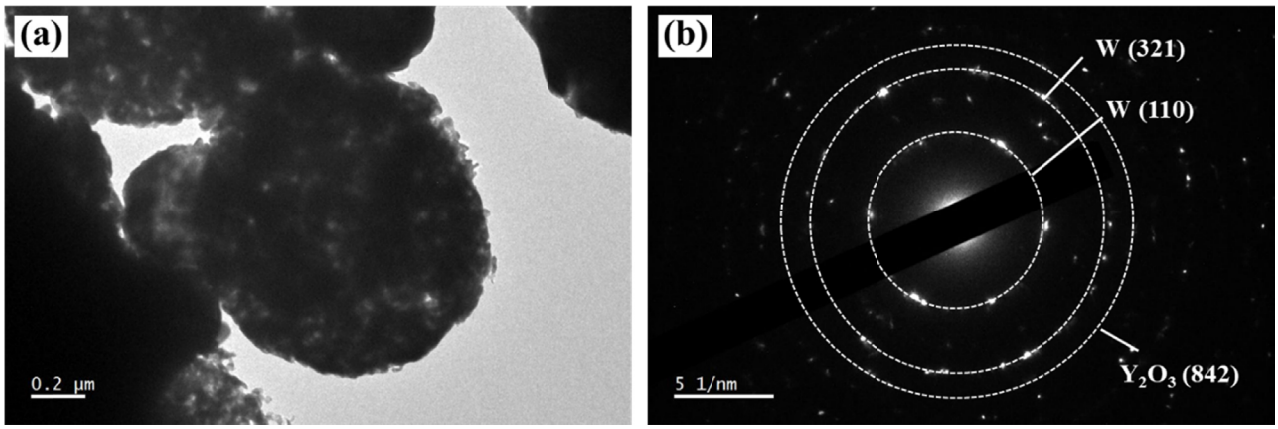

Fig. 5. (a) TEM image and (b) SAED patterns analysis of W-0.5wt% Y_2O_3 composite powder after calcination at 600°C for 5 h and hydrogen reduction at 800°C for 1 h

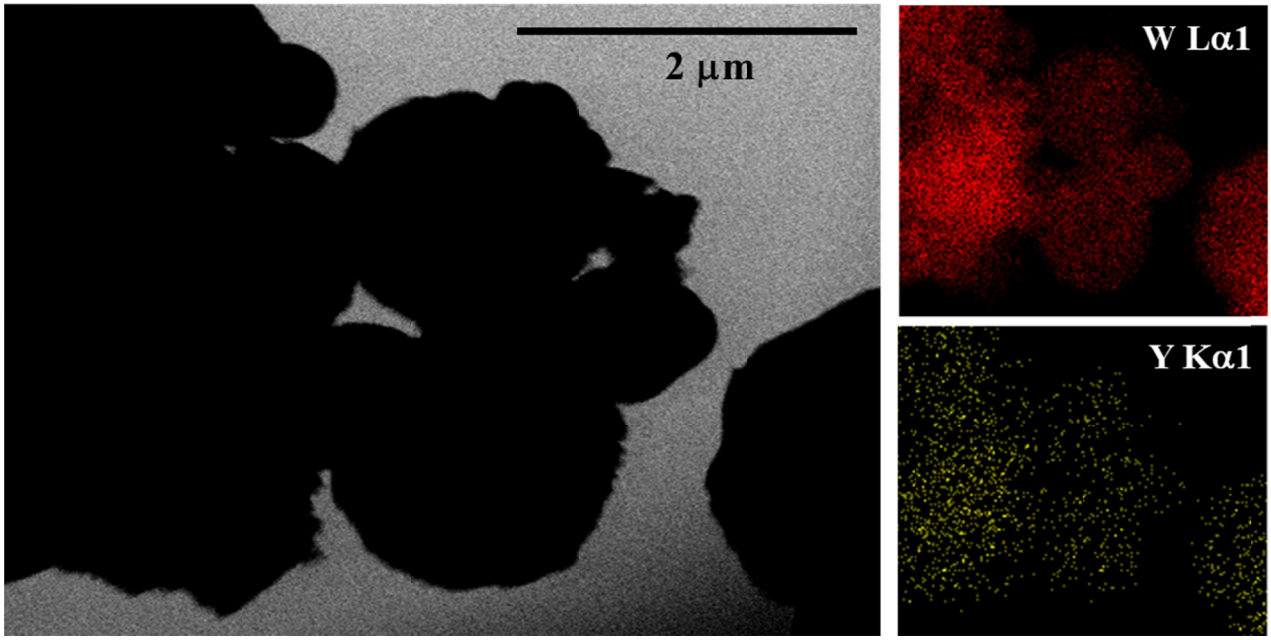

Fig. 6. TEM-EDS analysis of W-0.5wt% Y_2O_3 composite powder after calcination at 600°C for 5 h and hydrogen reduction at 800°C for 1 h

reveal the detailed microstructure of prepared powders, the distribution of alloy elements is characterized by TEM observation and EDX mapping, as shown in Fig. 6. It clearly represented a uniform distribution of Y element in the powder mixture. From these observations, it is suggested that the USP and polymeric additive solution route are useful for producing W powder with homogeneously dispersed Y_2O_3 nanoparticles.

4. Conclusions

This study was focused on the synthesis of W powders with homogenous dispersion of Y_2O_3 nanoparticles. The tungsten powders synthesized by the ultrasonic spray pyrolysis and hydrogen reduction showed spherical particles less than 2 mm in size. The W composite powder with 0.5 wt% Y_2O_3 nanoparticles was prepared by a polymer addition solution method using powder mixture of hydrogen-reduced W, Y-nitrate and PVA. TEM and phase analysis revealed that the W powder with a uniform distribution of Y_2O_3 nanoparticles can be produced by the further hydrogen reduction of calcined powder mixture. These results indicated that ultra-fine Y_2O_3 particles dispersed W composite powders can be fabricated by using ultrasonic spray pyrolysis and polymeric additive solution method.

Acknowledgments

This work was supported by the National Research Foundation of Korea (NRF) grant funded by the Korea government (MSIT) (2019R1A2B5B01070587).

REFERENCES

[1] W.D. Klopp, J. Less-Common Met. **42**, 261 (1975).
[2] V. Philipps, J. Nucl. Mater. **415**, S2 (2011).
[3] L. Veleva, Z. Oksiuta, U. Vogt, N. Baluc, Fusion Eng. Des. **84**, 1920 (2009).
[4] Z. Dong, N. Liu, Z. Ma, C. Liu, Q. Guo, Y. Liu, J. Alloys Compd. **695**, 2969 (2017).
[5] C. Ren, Z.Z. Fang, M. Koopman, B. Butler, J. Paramore, S. Middlemas, Int. J. Refract. Met. Hard Mater. **75**, 170 (2018).
[6] M.H. Nguyen, S.-J. Lee, W.M. Kriven, J. Mater. Res. **14**, 3417 (1999).
[7] S. Yan, J. Yin, E. Zhou, J. Alloys Compd. **450**, 417 (2008).
[8] T.R. Wilken, W.R. Morcom, C.A. Wert, J.B. Woodhouse, Met. Trans. B **7**, 589 (1976).
[9] S.C. Cifuentes, M.A. Monge, P. Pérez, Corros. Sci. **57**, 114 (2012).